Supplement of

Molecular dynamics study on the liquid-liquid contact angle in liquid-liquid phase separated aerosols

Chao Zhang et al.

Correspondence to: Yang Yang (yangyang@usst.edu.cn)

1. Simulation details

All molecular dynamics simulations in this study were conducted using LAMMPS (Plimpton, 1995). The droplet compositions were dodecane + water, dodecane + water + sodium chloride (NaCl), and dodecane + water + suberic acid, respectively. In the Martini force field, a dodecane molecule was mapped to standard C1 beads, with each C1 bead containing four carbon atoms (Fig. S1). Water molecules were mapped to uncharged P4 beads in the Martini force field, with each bead containing four water molecules. A special "anti-freezing" bead (BP4) was introduced to prevent water from freezing at around 300 K. Sodium and chloride ions were represented by Q_a and Q_d beads, respectively. In the OPLS-UA force field, each $-CH_3$ and $-CH_2$ group was represented by a single particle, and water molecules were modeled using the SPC/E model (Berendsen et al., 1987), which can be adopted to accurately predict key physicochemical properties of water, especially its density and surface tension (Zhang et al., 2025; Zhang et al., 2024). The SPC/E model is suitable for various water-based

simulations and is widely used in the study of water phase transition simulations and water cluster microstructures (Li and Bourg, 2023). NaCl was parameterized using parameters developed by Dang (1995).

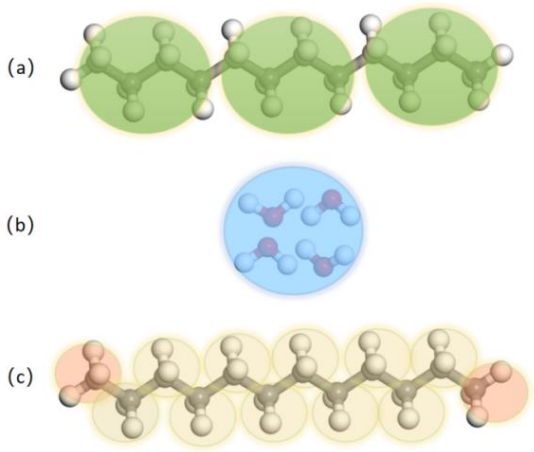

Fig. S1 Mapping schemes of Martini force field and united atom force field: (a) Martini model of dodecane using 1-4 mapping scheme; (b) Martini model of water using 1-4 mapping scheme; (c) UA model of dodecane with groups represented by single particles

The interaction forces between different beads in the Martini force field are expressed as follows:

$$U_{tot} = \sum_{nonbond}\left[4\varepsilon_{ij}\left(\frac{\sigma_{ij}^{12}}{r_{ij}^{12}}-\frac{\sigma_{ij}^{6}}{r_{ij}^{6}}\right)+\frac{q_i q_j}{r_{ij}}\right] + \sum_{bond}\frac{1}{2}K_{bond}\left(R-R_{bond}\right)^2+\sum_{angle}\frac{1}{2}K_{angle}\left[\cos(\theta)-\cos(\theta_0)\right]^2 \quad (1)$$

where the three terms on the right side of the equal sign are energies of non-bonding interactions including Lennard-Jones term and the Coulomb term, bond stretching, angle bending, ε_{ij} is the energy parameter of the interaction, σ_{ij} is the Lennard-Jones core diameter, r is the distance between two beads (i and j), and q is the charge of the bead, R, R_{bond} and K_{bond} are the distance between two beads, the equilibrium distance between these two beads, and the bond potential energy constant, and θ and K_{angel} are

the bond angle and the angular potential energy constant. Parameters of the Martini force field are listed in Table S1-S3.

In the OPLS-UA force field, the interaction between different particles is expressed as:

$$U_{tot} = \sum_{nonbond}\left[4\varepsilon_{ij}\left(\frac{\sigma_{ij}^{12}}{r_{ij}^{12}}-\frac{\sigma_{ij}^{6}}{r_{ij}^{6}}\right)+\frac{q_i q_j}{r_{ij}}\right] f_{ij} + \sum_{bond} K_b\left(b-b_0\right)^2 + \sum_{angle} K_\theta\left(\theta-\theta_0\right) + \sum torsion\left\{\frac{V_1}{2}\left[1+\cos\left(\phi\right)\right]+\frac{V_2}{2}\left[1-\cos\left(2\phi\right)\right]+\frac{V_3}{2}\left[1+\cos\left(3\phi\right)\right]+\frac{V_4}{2}\left[1-\cos\left(4\phi\right)\right]\right\} \quad (2)$$

where the four terms on the right side of the equation are the energies of non-bonding interactions, bond stretching, angle bending and torsion, respectively. The non-bonding interaction term consists of the Lennard-Jones term and the Coulomb term, which are used for the non-bonding interactions between atoms in different molecules and within a molecule where the two atoms are separated by three or more bonds (f_{ij} = 0.5) or more (f_{ij} = 1.0). V_i is the Fourier coefficient and ϕ is the dihedral angle. Parameters of the OPLS-UA force field are listed in Table S4-S7.

In the simulations based on the Martini force field, non-bonded interactions were truncated at a distance of r_c = 1.2 nm. Moltemplate was used to establish the initial droplet models. In the united-atom OPLS-UA force field simulations, the LJ interaction cutoff distance was set to 1.4 nm, and the PPPM method was used to calculate the long-range Coulombic interactions. The interactions between different atoms in the force field were calculated using the Lorenz-Berthelot (LB) combination rule 41, where $\varepsilon_{ij} = (\varepsilon_i\varepsilon_j)^{1/2}$ and $\sigma_{ij} = (\sigma_i + \sigma_j)/2$. The time step was set to 5 fs, and the SHAKE algorithm was used to fix the bond angles and bond lengths of SPC/E water. The simulation process adopted the NVT ensemble, and the temperature was controlled by the Nose-Hoover

thermostat. In simulations based on the Martini force field, the system temperatures were controlled to 240 K, 260 K, 280 K, 300 K, and 320 K, respectively, with a time step of 20 fs. In simulations based on the OPLS-UA force field, the simulation temperatures were 280 K, 290 K, 300 K, 310 K, and 320 K, respectively. The system with a temperature below 280 K is not simulated because at low temperatures irregular dodecane cluster shapes can lead to significant deviations in the contact angle calculation. At the initial simulation moment, all systems were energy minimized using the steepest descent method to eliminate any close contacts between particles or beads. The equilibrium state of the system was determined by tracking the changes in system energy. After reaching equilibrium, the positions of all atoms were statistically recorded every 2 ps for a total of 3 ns.

Table S1. Parameter values for the non-bond interaction in the Martini force field

	σ(Å)	ε(kcal/mol)	q(e)
C1	4.7	0.836521	0
P4	4.7	1.195030	0
BP4	4.7	1.195030	0
Q_a	4.7	1.195030	-1
Q_d	4.7	1.195030	1

Table S2. Parameter values for the bond-stretching interaction in the Martini force field

	K_{bond}(kcal/mol·Å^2)	$\mathbf{R}_{bond}$(Å)
C1-C1	1.493787	4.7

73

74 Table S3. Parameter values for the bond angle bending interactions in the Martini force field

	K_{angle}(kcal/mol·Å^2)	θ_0(°)
C1-C1-C1	2.987575	180

75

76 Table S4. Parameter values for the non-bond interaction in the OPLS-UA force field

	σ(Å)	ε(kcal/mol)	q(e)
-CH_3	3.905	0.175	0
-CH_2	3.905	0.118	0
-C	3.75	0.105	0.55
-O	3	0.17	-0.58
=O	2.96	0.21	-0.5
-H	0	0	0.45
-CH_2	3.905	0.118	0.08
-CH_2	3.905	0.118	0

-Cl	4.401	0.0999	-1
-Na	2.584	0.0999	1
-H	0	0	0.4238
-O	3.166	0.1553	-0.8476

Table S5. Parameter values for the bond-stretching interaction in the OPLS-UA force field

	K_b(kcal/mol·Å^2)	R_b(Å)
CH_3-CH_2	260	1.526
CH_2-CH_2	260	1.526
C-O	450	1.364
C=O	570	1.214
C-CH_2	317	1.52
H-O	553	0.97
H-O	450	1.0

Table S6. Parameter values for the bond angle bending in the OPLS-UA force field

	K_θ(kcal/mol·Å^2)	θ_0(°)
CH_3-CH_2-CH_2	63	112.4
CH_2-CH_2-CH_2	63	112.4
O-C=O	80	123
O-C-CH_2	70	111
O=C-CH_2	80	126
C-O-H	35	107
C-CH_2-CH_2	63	112.4
H-O-H	55	109.47

Table S7. Parameter values for the torsional (dihedral angles) interactions in the OPLS-UA force field

	V_1	V_2	V_3	V_4
CH_3-CH_2-CH_2-CH_2	-3.4	1.25	3.1	0
CH_2-CH_2-CH_2-CH_2	-3.4	1.25	3.1	0
CH_2-CH_2-C-O	0	1.412	0	0
CH_2-CH_2-C=O	0	0	0	0

CH_2-CH_2-CH_2-C	-2.06	-0.313	0.315	0

2. Results and Discussion

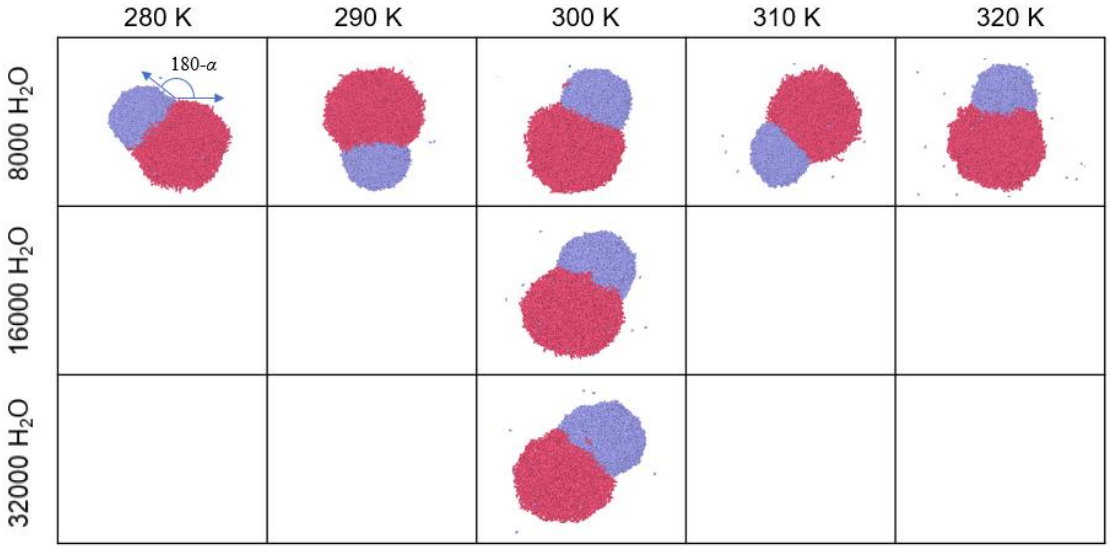

Fig. S2 Snapshots of water-dodecane droplets under different temperatures and water contents (MD simulations with OPLS-UA field）, dodecane and water molecules are represented by red and blue balls, respectively

Table S8. Fitting parameters in equation (9) for all systems

Case	*a*1	*a*2	*a*3	*a*4	*a*5
water-dodecane (Martini)	5.82×10^{3}	8.36×10^{1}	-0.448	0.1×10^{-2}	-9.42×10^{-7}
water-dodecane (OPLS-UA)	7.19×10^{3}	-9.64×10^{2}	4.843	-0.011	9.02×10^{-7}

water-dodecane-NaCl `(Martini)	-3.92×10^{3}	5.83×10^{1}	-0.324	7.95×10^{-4}	-7.28×10^{-7}
water-dodecane-NaCl (OPLS-UA)	1.49×10^{5}	-1.99×10^{3}	9.982	-0.22×10^{-1}	1.85×10^{-5}
water-dodecane-suberic acid (OPLS-UA)	-7.53×10^{6}	9.96×104	-4.94×10^{2}	1.087	-8.98×10^{-4}

References

Berendsen, H. J., Grigera, J.-R., and Straatsma, T. P.: The missing term in effective pair potentials, J. Phys. Chem., 91, 6269-6271, 1987.

Dang, L. X.: Mechanism and thermodynamics of ion selectivity in aqueous solutions of 18-crown-6 ether: a molecular dynamics study, J. Am. Chem. Soc., 117, 6954-6960, 1995.

Li, X. and Bourg, I. C.: Microphysics of liquid water in sub-10 nm ultrafine aerosol particles, Atmos. Chem. Phys., 23, 2525-2556, 2023.

Plimpton, S.: Fast parallel algorithms for short-range molecular dynamics, J. Comput. Phys., 117, 1-19, 1995.

Zhang, C., Yu, D., Ma, N., and Wang, Y. J. P. T.: Effect of size and concentration

corrections for surface tension on the hygroscopicity prediction of nano-aerosols, 433, 119278, 2024.

Zhang, C., Lin, H., Zhang, Z., Yang, Y., Pan, J., Wang, Y., and Wiedensohler, A. J. P. o. F.: Quantitative description of surface tension for nanodroplets containing ammonium sulfate and its application to the particle hygroscopicity prediction, 37, 2025.